

Philosophical Magazine

Publication details, including instructions for authors
and subscription information:

<http://www.tandfonline.com/loi/tphm19>

On the ground state properties of the anisotropic triangular antiferromagnet

P. Fazekas^{a b} & P. W. Anderson^a

^a Cavendish Laboratory, Cambridge, England

^b Central Research Institute for Physics, H-1525
Budapest 114, P.O.B. 49, Hungary

Published online: 20 Aug 2006.

To cite this article: P. Fazekas & P. W. Anderson (1974) On the ground state properties of the anisotropic triangular antiferromagnet, *Philosophical Magazine*, 30:2, 423-440

To link to this article: <http://dx.doi.org/10.1080/14786439808206568>

PLEASE SCROLL DOWN FOR ARTICLE

Taylor & Francis makes every effort to ensure the accuracy of all the information (the "Content") contained in the publications on our platform. However, Taylor & Francis, our agents, and our licensors make no representations or warranties whatsoever as to the accuracy, completeness, or suitability for any purpose of the Content. Any opinions and views expressed in this publication are the opinions and views of the authors, and are not the views of or endorsed by Taylor & Francis. The accuracy of the Content should not be relied upon and should be independently verified with primary sources of information. Taylor and Francis shall not be liable for any losses, actions, claims, proceedings, demands, costs, expenses, damages, and other liabilities whatsoever or howsoever caused arising directly or indirectly in connection with, in relation to or arising out of the use of the Content.

This article may be used for research, teaching, and private study purposes. Any substantial or systematic reproduction, redistribution, reselling, loan, sub-licensing, systematic supply, or distribution in any form to anyone is expressly

On the ground state properties of the anisotropic triangular antiferromagnet

By P. FAZEKAS† and P. W. ANDERSON‡
Cavendish Laboratory, Cambridge, England

[Received 24 May 1974]

ABSTRACT

Our aim is to present further evidence supporting a recent suggestion by Anderson (1973) that the ground state of the triangular antiferromagnet is different from the conventional three-sublattice Néel state. The anisotropic Heisenberg model is investigated. Near the Ising limit a peculiar, possibly liquid-like state is found to be energetically more favourable than the Néel-state. It seems to be probable that this type of ground state prevails in the anisotropy region between the Ising model and the isotropic Heisenberg model. The implications for the applicability of the resonating valence bond picture to the $S = \frac{1}{2}$ antiferromagnets are also discussed.

§ 1. INTRODUCTION

It has been suggested recently (Anderson 1973) that the ground state of some $S = \frac{1}{2}$ Heisenberg antiferromagnets may be quite different from the conventional Néel-state characterized by large sublattice magnetizations. Until quite recently experimental evidence for the Néel-type antiferromagnetic state in $S = \frac{1}{2}$ materials had been quite scarce; and in the few cases that were known as such it may have been ascribable to a large anisotropy. On the theoretical side, ever since the exact solution of the linear chain problem by Bethe (1931) there has been a lingering doubt that the actual ground state may be liquid-like, with no preferred spin direction at a given lattice site. Bethe's solution certainly does not have sublattices and possibly not even the internal correlations characteristic of the antiferromagnetic state. Marshall (1955) argued that the ground state is disordered in certain two-and-three-dimensional two-sublattice cases as well. However, as Thouless (1967) pointed out, the correlations characteristic of the antiferromagnetic order are present in Marshall's (1955) variational wavefunction, though not in an easily recognizable form as the magnetizations lie in the plane perpendicular to the quantization direction.

Hulthén's (1938) cluster approach provided a pictorial way of thinking about this hypothetical non-magnetic ground state: it can be envisaged as a linear combination of wave functions built up of singlet pairs. We may think of it as of a liquid-type state in which the system of pair bonds is resonating

† Permanent address: Central Research Institute for Physics, H-1525 Budapest 114, P.O.B. 49, Hungary.

‡ Also at Bell Laboratories, Murray Hill, New Jersey 07974, U.S.A.

between the possible configurations. Anderson (1973) applied Hulthén's method to get a variational estimate for the ground-state energy of the triangular antiferromagnet described by the Hamiltonian

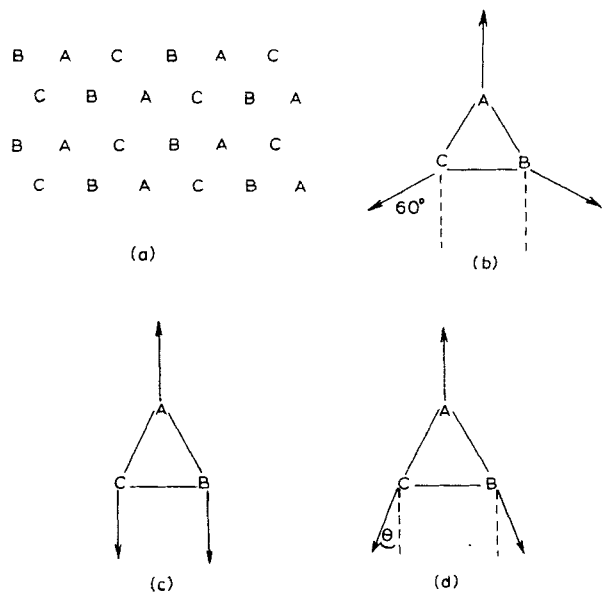
$$H = J \sum_{\langle i,j \rangle} \mathbf{S}_i \cdot \mathbf{S}_j, \tag{1}$$

where $J > 0$ and $\langle i,j \rangle$ refers to the nearest-neighbour pairs. He obtained the result

$$E_{\text{gr}} \sim -0.54NJ, \tag{2}$$

where N is the number of lattice sites. This should be compared with the energy of the best (three-sublattice) Néel-state (fig. 1 (a)-(b)) the result for which was given as $-0.463NJ$. As (2) is much lower than the spin-wave result, Anderson (1973) postulated that the ground state in this case may be a non-magnetic, probably disordered, so-called resonating-valence-bond (RVB) state, while the Néel state is only metastable. However, because of the uncertainty in the spin-wave result and the almost complete lack of information about the character of the RVB state one may have entertained the doubt that we are merely confronted with two approximations to the energy of the same (Néel-type) state.

Fig. 1



The three-sublattice Néel state : (a) the sublattices. The directions of sublattice magnetizations for (b) $\alpha = 1$; (c) $\alpha = 0$; (d) $0 < \alpha < 1$.

In the next section we set up variational trial wave functions for the ground state of the anisotropic triangular antiferromagnet. For large anisotropies these will be shown to have lower energies than the Néel-state, and they are quite competitive with the Néel-state even in the isotropic case. Section 3 discusses the information gained about the other features of these wave

functions. In the fourth section second-order perturbation theory is applied to improve upon the energy estimates obtained previously. In the conclusion we comment on the general relevance of our results to the problem whether non-Néel type ground states are likely to occur in $S = \frac{1}{2}$ systems.

§ 2. VARIATIONAL RESULTS FOR THE GROUND-STATE ENERGY

The aim of the present paper is to supply further evidence that the triangular antiferromagnet is likely to have a ground state which is different from that shown in fig. 1 (b). The motivation for the existence of such a state becomes clearer if we examine the anisotropic Heisenberg model

$$H = H^z + H^\pm = J \sum_{\langle i, j \rangle} S_i^z S_j^z + J \frac{\alpha}{2} \sum_{\langle i, j \rangle} (S_i^+ S_j^- + S_j^+ S_i^-), \quad (3)$$

with $1 \geq \alpha \geq 0$. A peculiar non-Néel-type state is the most conspicuous in the $\alpha \ll 1$ limit and, according to our estimate, it can be continued as ground state up to $\alpha = 1$, the case investigated by Anderson (1973).

First, let us consider the Néel-state. As one of us (Anderson, to be published) pointed out, the best one is probably that which with increasing α gradually transforms into the 120° state (fig. 1 (b)). One starts with a particular Ising ground state which already has the same sublattices (fig. 1 (c)). For small α s the B and C sublattice magnetizations tilt with the angle θ (fig. 1 (d)), where from the minimization of the classical energy E_{cl}

$$\cos \theta = \frac{1}{1 + \alpha},$$

θ varying from 0° to 60° as α increases from 0 to 1, and

$$\frac{1}{N} E_{cl} = -JS^2 \frac{1 + \alpha + \alpha^2}{1 + \alpha}, \quad (4)$$

S being the spin. For small α 's the energy gain with respect to the energy of the Ising state $E_{\text{Ising}} = -JS^2N$, is quadratic in α

$$\frac{1}{N} E_{cl} \approx \frac{1}{N} E_{\text{Ising}} - JS^2 \alpha^2, \quad (4a)$$

A similar conclusion could be drawn from the quasi-classical spin wave calculation based on the three-sublattice state shown in fig. 1 (d).

In what follows we will be speaking only of the $S = \frac{1}{2}$ case. Our argument in favour of a non-Néel-type state rests on the recognition that it is possible to construct states whose energy depends linearly on α

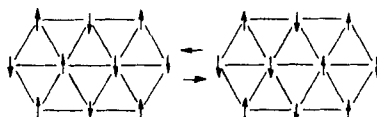
$$\frac{1}{N} E_{tr} = \frac{1}{N} E_{\text{Ising}} - b\alpha, \quad (5)$$

where E_{tr} is the energy of our respective trial wave functions.

The reason for this is the following. When $\alpha = 0$ (Ising model) the ground-state manifold has a zero point entropy, there being a macroscopic number of states with exactly the minimum number of nearest-neighbour parallel pairs

(Wannier 1950). We shall call them short-range ordered (SRO) states. An easy way to characterize them is to say that they contain no unit triangle with three parallel spins. For small α s we can expect that the spin-flip term H^\pm lifts the degeneracy of the SRO states, making some linear combination of them the most favourable. As H^\pm has matrix elements between certain SRO states (not all of them, but the statement is true of a set of states itself having zero-point entropy) the corresponding energy correction is bound to be linear in α .

Fig. 2



Interchangeable pair.

Figure 2 shows a ten-site cluster which can be regarded as part of a SRO configuration and the central pair of which can be interchanged without breaking the SRO. We shall refer to such a pair as an interchangeable pair (IP). The surrounding eight sites have to have this configuration (or the trivially different one obtained by replacing up spins with down spins and vice versa) in order to make the spin flip process non-SRO-breaking.

For every IP we can gain an energy $-(\alpha/2)$ as follows. If the members of the IP are spins 1 and 2, we use the singlet linear combination for them

$$\Psi = \Psi_{\text{Ising}}(m=3, 4, \dots) \frac{\alpha_1\beta_2 - \alpha_2\beta_1}{\sqrt{2}}$$

and

$$\left(\frac{\alpha_1\beta_2 - \alpha_2\beta_1}{\sqrt{2}} \middle| S_1^z S_2^z + \frac{\alpha}{2} (S_1^+ S_2^- + S_2^+ S_1^-) \middle| \frac{\alpha_1\beta_2 - \alpha_2\beta_1}{\sqrt{2}} \right) = -\frac{1}{4} - \frac{\alpha}{2}.$$

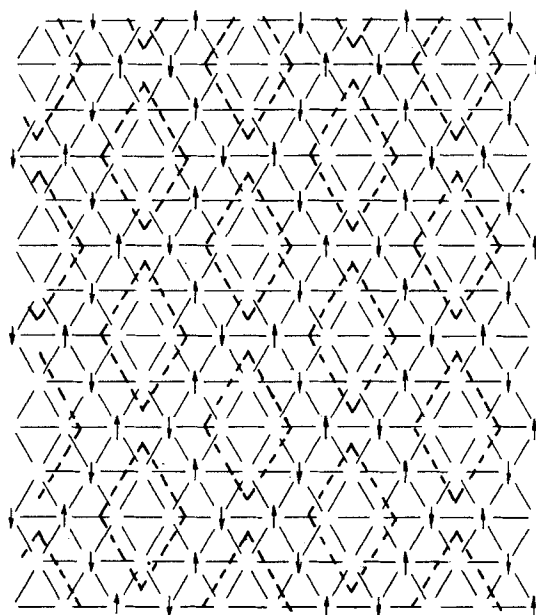
Obviously, for $\alpha \ll 1$ the ground state has to have as many IPs as possible. An example of a state with a high concentration of IPs is shown in fig. 3. Half of the spins ($N/4 \downarrow$ spins, $N/4 \uparrow$ spins) are held fixed along the boundaries of eight-site clusters. The other half of the spins, situated within the diamond-shaped cells (dashed lines) are described by a linear combination of the four configurations shown in fig. 4. (Actually, there are two different types of cells but one can be obtained from the other by $\uparrow \rightleftharpoons \downarrow$ replacement.) The proposed wavefunction is

$$\Psi_{\text{tr}} = \Phi_{\text{bg}} \prod_{i=1}^{N/8} \frac{\phi_{i1} - \phi_{i2} + \phi_{i3} - \phi_{i4}}{2}. \quad (6)$$

Here Φ_{bg} describes the 'solid background' of the $N/2$ spins on the cluster boundaries, and $\phi_{i1}, \dots, \phi_{i4}$ are the four possible states of the spins within the i th cell. The corresponding energy is

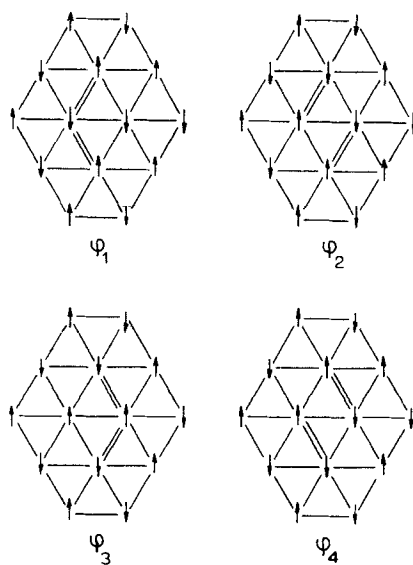
$$\frac{1}{NJ} E_{\text{tr}} = \frac{1}{NJ} \langle \Psi_{\text{tr}} | H | \Psi_{\text{tr}} \rangle = -0.25 - 0.125\alpha. \quad (7)$$

Fig. 3



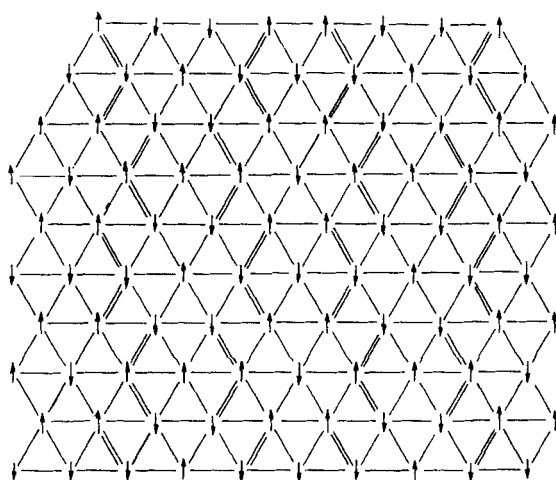
The state described in eqn. (6). The spins forming the 'solid background' are shown. The cells framed by dashed lines are in a linear combination of the states shown in fig. 4.

Fig. 4



The four SRO configurations of a cluster. IPs are indicated with double lines.

Fig. 5



One of the configurations with the maximum number of IPs.

With (6) and (7) we have demonstrated that it is possible to construct a state, which, taking advantage of the existence of the IPs, has an energy term linear in α , and for which the coefficient of α is of the same order of magnitude as the constant term. The linearity in itself already makes the state superior to the Néel state for very small α s, but the latter feature is also essential if we want it to be competitive with the Néel state near $\alpha = 1$. Otherwise it is clear that (6) is rather different from what we expect the ground state to be like. The 'solid background' comprising half of the lattice is merely an artifact dictated by computational convenience as it gives the chance to treat the clusters independently. The price to be paid for this is that only $\frac{1}{12}$ of the nearest-neighbour pairs are interchangeable. Figure 5 shows a configuration which seems to provide a much better starting point for the ground state as it has twice as many IPs. We have not been able to find better configurations but it is easy to show that there are many others in which, like in the one in fig. 5, $\frac{1}{6}$ of the pairs are IPs. Most of these configurations do not have long-range order. Accepting that we cannot do better than in fig. 5, we get an upper limit for b

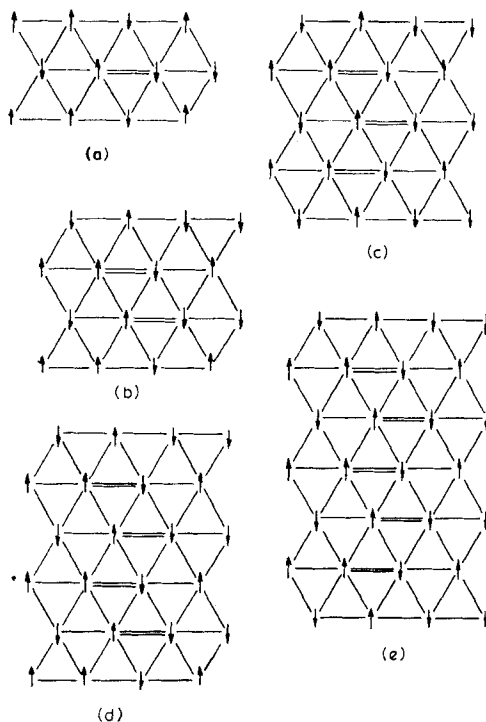
$$b < \frac{1}{N\alpha} \cdot 3N \cdot \frac{1}{6} \cdot \frac{\alpha}{2} = 0.25.$$

It is easy to see that the upper limit cannot be achieved. If we interchange one of the IPs in fig. 5, four others cease to exist. States with a large number of IPs have matrix elements mainly to states with fewer IPs, thereby reducing the ground-state averaged concentration to a value below $\frac{1}{6}$.

Undoubtedly, to get a good approximation to the ground state one should start from states like that in fig. 5, and letting H^\pm act on the IPs, mix the resulting configurations as well, etc. But just because of the large concentration of IPs the lattice cannot be divided into independent parts; there is no 'solid background' with fixed spins and the ground state is likely to have liquid-like properties. We have not been able to give explicit prescription for

such a ground-state wave function. Nevertheless, it is plausible that by increasing the size of the clusters in states like (6) we can gradually decrease the proportion of the spurious solid background and so we may be able to get an improved variational estimate for b . We also hope to find some regularity in the behaviour of the 'liquid part' within the clusters.

Fig. 6

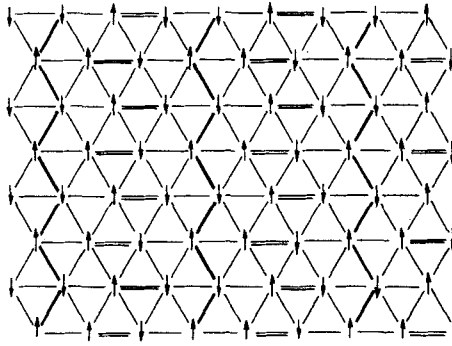


Clusters for trial wave functions.

We have chosen the series of clusters shown in figs. 6 (a)–(e). They represent successive approximations to the state in which the whole plane is cut into zig-zag stripes as shown in fig. 7. For the inside of the stripes one particular configuration with the maximum number of IPs is shown. We see that, given the constraint of fixed spins on boundary sites, even the best configuration is worse than that shown in fig. 5 because the concentration of IPs is only $\frac{1}{9}$. (We cannot count pairs with one endpoint on the borderline of a stripe as these cannot be interchanged.) Consequently, we can expect that $b_{\text{stripe}} < 0.167$ but hopefully it is larger than 0.125.

The clusters in figs. 6 (a), (c) and (e) can immediately be stacked upon each other to form the zig-zag stripes and thus can be used to cover the whole lattice. In the cases shown in figs. 6 (b), (d) we have to use the twins of the clusters which can be obtained by slicing the stripe one step higher. But these are energetically equivalent to those shown and do not necessitate extra calculations.

Fig. 7



The division of the lattice into zig-zag stripes.

All the cluster trial wave functions have a form like (6)

$$\Psi_{\text{tr}} = \Phi_{\text{bg}} \prod_{i=1}^{N/m} \left(\sum_{\mu} c_{i\mu} \phi_{i\mu} \right).$$

Here Φ_{bg} described the spins held fixed along the boundaries, and the product is over the N/m clusters, where m is the number of sites per cluster. The wave function for the inside of a cluster is obtained in the following way: we start from one of the configurations having the maximum number of IPs inside the cluster (such are shown in figs. 6 (a)–(e) and let H^{\pm} act on the IPs. By this means we generate the complete set of wave functions available from the starting one exchanging only IPs, and then we diagonalize H^{\pm} in this set. Denoting the lowest eigenvalue by ϵ_m we get for the ground-state energy resulting from the trial wave function with m -site clusters $E_{\text{gr}}(m)$

$$\frac{1}{N} E_{\text{gr}}(m) = \frac{1}{N} E_{\text{Ising}} + \frac{1}{m} \epsilon_m.$$

Considering that the clusters contain 6, 9, 12, 15, 18 sites, respectively, the ground-state energy per site is found to be

$$\frac{1}{N} E_{\text{gr}}(6) = -0.25J - 0.0833\alpha J, \quad (8a)$$

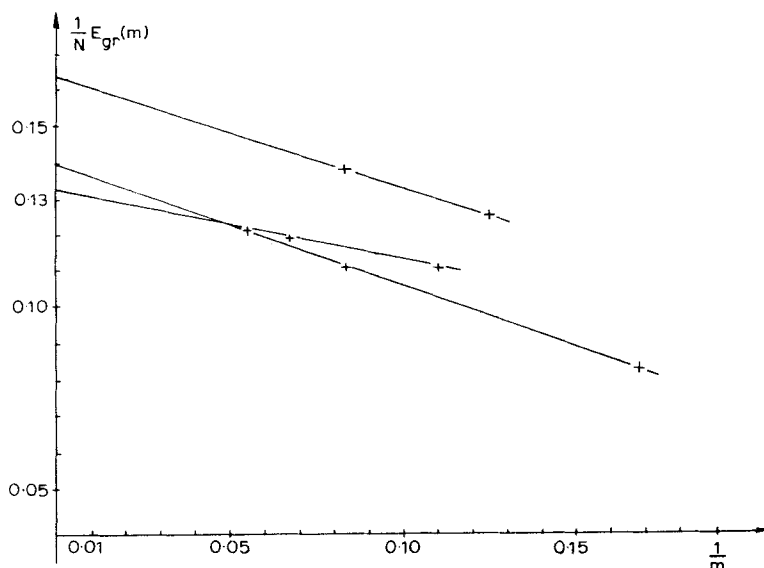
$$\frac{1}{N} E_{\text{gr}}(9) = -0.25J - 0.1111\alpha J, \quad (8b)$$

$$\frac{1}{N} E_{\text{gr}}(12) = -0.25J - 0.1104\alpha J, \quad (8c)$$

$$\frac{1}{N} E_{\text{gr}}(15) = -0.25J - 0.1190\alpha J, \quad (8d)$$

$$\frac{1}{N} E_{\text{gr}}(18) = -0.25J - 0.1216\alpha J. \quad (8e)$$

Fig. 8



The extrapolation of b values from cluster results. The upper line refers to the clusters in figs. 3 and 9, the lower lines to the clusters in fig. 6.

None of these supersedes (7). But the value estimated for the stripe-wave function (fig. 7) is already slightly better. Supposing that

$$\frac{1}{N} E_{\text{gr}}(m) \approx \frac{1}{N} E_{\text{gr}}(\text{stripe}) - \frac{d}{m},$$

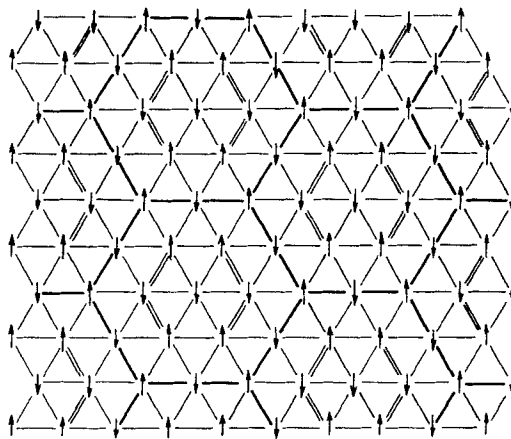
we can estimate $(1/N)E_{\text{gr}}(\text{stripe})$ by plotting $(1/N)E_{\text{gr}}(m)$ versus $1/m$ (fig. 8). An odd-even effect is noticeable. Roughly speaking we get

$$b_{\text{stripe}} \sim 0.135 - 0.14. \quad (9)$$

This is already an improvement upon (7) but it does not take us anywhere near the energy needed to supersede the Néel state at $\alpha = 1$. But, as we have said, 0.14 should be compared to 0.167, of which it falls short only by $\sim 15\%$. It is also obvious that we can make a much better start. For example, the 12-atom cluster shown in fig. 9 gives $b \sim 0.138$, about the same as the infinite stripes. If we take the clusters in figs. 3 and 9 as the two first approximations to the four-row thick slab, the b value estimated for that is already ~ 0.164 (fig. 8).

The data listed above give us a sort of a numerical experience which can be used to make a guess at the b value corresponding to the real ground state. Let us define the effective number of IPs for m -site clusters as $b(m) = -(2\epsilon_m/\alpha J)$. For large enough clusters as in figs. 6 (c)–(e) and 9, and also for the zig-zag stripe, we find that this effective value is about 15–20% less than that corresponding to a ‘best’ configuration. If we assume that a similar reduction

Fig. 9



Hexagonal clusters for a trial wave function. For the inside of the cluster one of the 'best' configurations is shown.

occurs if we start from, e.g. the state in fig. 5, for the supposedly true ground state derived from that we get

$$b_{\text{gr}} \sim 0.20 - 0.21. \quad (10)$$

Should this estimate be reliable, the corresponding ground-state energy for $\alpha = 1$ would be

$$E_{\text{gr}} \sim -0.46JN, \quad (11)$$

i.e. about as good as the spin wave result. In the isotropic case the wave function has to be augmented with a fair number of SRO-breaking configurations, reducing the energy (as we shall see in § 4) still further. This gives grounds to expect that a state which is the continuation of the ground state valid for $\alpha \ll 1$, i.e. which is characterized by a certain predominance of IPs, will be the ground state even at $\alpha = 1$.

§ 3. ON THE NATURE OF THE CLUSTER WAVEFUNCTIONS

The approach presented in the previous section, while it gives some information on the ground state energy, is less enlightening about the nature of the hypothetical RVB ground state. In particular, it cannot prove or disprove the presence of some form of DLRO or ODLRO. However, two hints can be gained from the inspection of the cluster ground-state wavefunctions. One of them is an obvious tendency for 'liquidity', i.e. no definite spin direction for a given site, and also for a particular many-site short-range correlation because of the prevalence of the configuration shown in fig. 2. The other feature of which we learned empirically, is the probable existence of a long-range phase coherence. We noticed that, at least for the clusters examined by us, whenever two SRO states are connected by a matrix element of H^\pm , they have opposite signs in the expansion of the ground state. This implies

that if, with interchanging IPs only, we can get from the SRO state α to SRO state β via two different sequences of states

$$\alpha \rightarrow \phi_1 \rightarrow \dots \rightarrow \phi_{m-1} \rightarrow \beta,$$

$$\alpha \rightarrow \psi_1 \rightarrow \dots \rightarrow \psi_{n-1} \rightarrow \beta,$$

then m and n are either both odd or both even. In this general form the above statement is merely a guess which we have not been able to prove but for which we have found supportive evidence by examining certain specific ways of getting from state α to state β . These arguments are presented in the Appendix. Conversely, if the above guess turns out to be correct, the RVB ground-state wave function can be sought in the form

$$\Psi_{\text{gr}} = \sum_{\mu} (-1)^{p_{\mu}} c_{\mu} \phi_{\mu}$$

where the summation is over the SRO states, $c_{\mu} \geq 0$, and $p_{\mu} = p_{\mu} - p_{\mu}$ is the number of IP interchanges needed to reach the state ϕ_{μ} from ϕ_{μ} . According to our assumption the parity of this number is well defined, i.e. it does not depend on the particular route we choose.

§ 4. SECOND-ORDER PERTURBATION THEORY

Up to this point we have treated the spin-flip term as a very small perturbation which mixes only the SRO states. However, as α becomes finite, the ground state will have an SRO-breaking component. The resulting energy correction is likely to be appreciable by the time we reach $\alpha = 1$.

In this section we make an attempt to estimate the second-order contribution to the ground-state energy. This is bound to be rather rudimentary as we do not have detailed knowledge of the ground-state wave function.

Let us start from the Ising state shown in fig. 1 (c). H^{\pm} acts on the $2N$ non-interchangeable antiparallel pairs (NIAPs) ('non-interchangeability' is to be understood in the context of § 2, i.e. that interchange leads to SRO breaking). Each of the resulting excited states has an energy higher by $2J$ than the Ising energy, as four antiparallel pairs are replaced by parallel ones. So the energy correction is

$$\Delta E^{(2)} = -2N \left(\frac{\alpha}{2} \right)^2 J^2 \frac{1}{2J} = -0.25\alpha^2 NJ,$$

in agreement with the expansion of E_{cl} (4 a).

Perturbing other SRO states, and for the moment disregarding the IPs, the energy correction will be rather similar. The number of NIAPs is always between $\frac{3}{2}N$ and $2N$; the energy denominators can take the values J , $2J$ and $3J$. The correction to the energy of the state shown in fig. 5 would be slightly larger, $\sim -0.26\alpha^2 NJ$, because of the predominance of smaller energy denominators. As the Ising state has no IPs, and the latter has the maximum number of them, we can assume that $\Delta E^{(2)}$ would be roughly the same for every SRO state.

However, this is likely to overestimate, perhaps severely, the second-order correction to the ground-state energy

$$\Delta E_{\text{gr}}^{(2)} = \sum \frac{|\langle \psi_i^0 | H^\pm | \psi_{\text{gr}}^0 \rangle|^2}{E_{\text{gr}}^0 - E_i^0} = \sum_i \frac{|\sum_\mu c_\mu \langle \psi_i^0 | H^\pm | \phi_\mu \rangle|^2}{E_{\text{gr}}^0 - E_i^0},$$

where ψ_{gr}^0 is the ground state represented as a linear combination of SRO states

$$\psi_{\text{gr}}^0 = \sum_\mu c_\mu \phi_\mu,$$

the ψ_i^0 s are the zeroth-order SRO breaking states, and E_{gr}^0 and E_i^0 the respective energies calculated with $\alpha=0$.

As we shall see, some of the ψ_i^0 s have matrix elements to more than one SRO state, and there is a tendency for cancellation, resulting in a reduction of $\Delta E^{(2)}$ from its naive value $\sim -0.25\alpha^2 JN$.

First let us examine the correction to the energy of the trial wave function (6). There are three different types of NIAPs and corresponding excited states :

(a) Those lying along the cluster boundaries. Here each excited state can be generated only in one way—from a well-defined SRO state by interchanging a well-defined NIAP. Therefore no cancellation can arise. We can estimate the energy correction by taking the number of such pairs ($5N/8$) and an average energy denominator ($2J$) giving

$$-\frac{5N}{8} \left(\frac{\alpha J}{2} \right)^2 \frac{1}{2J} \sim -0.08N\alpha^2 J.$$

(b) Pairs entirely within a cell (see fig. 3, cells are framed by dashed lines). This demonstrates the cancellation effect most clearly. As we can see in fig. 4, the average number of NIAPs per cell is $3/2$, so we should get

$$-\frac{N}{8} \cdot \frac{3}{2} \left(\frac{\alpha J}{2} \right)^2 \frac{1}{J} = -\frac{3}{64}\alpha^2 NJ.$$

Here $N/8$ is the number of cells in the lattice, and the excitation energy in this case is only J . By looking at the two SRO-breaking states ψ_1 and ψ_2 (fig. 10) we see that both of them couple to three SRO states : ψ_1 to ϕ_1, ϕ_2, ϕ_3 and ψ_2 to ϕ_1, ϕ_3 and ϕ_4 (see fig. 4), leading to

$$-\frac{N}{8} \frac{1}{J} \frac{1}{4} \sum_{i=1}^2 |\langle \phi_1 - \phi_2 + \phi_3 - \phi_4 | H^\pm | \psi_i \rangle|^2 = -\frac{1}{64}N\alpha^2 J = -0.015\alpha^2 NJ,$$

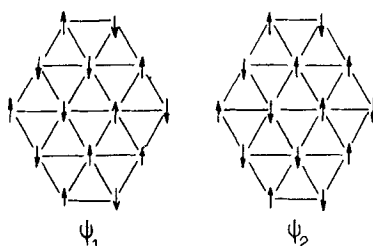
i.e. there is a reduction by a factor of three when compared to the naive estimate.

(c) Pairs connecting a border site with an inner site. There are 26 resulting excited states, four of them coupling to two different SRO states ; the contribution of these latter is zero. So cancellation occurs, though only to a much smaller extent than in case (b). The result—once again taking $2J$ for the average energy denominator—is $\sim -0.09\alpha^2 NJ$.

Altogether we have $\Delta E^{(2)} \simeq -0.185\alpha^2 NJ$.

One may be tempted to regard this as an estimate for the correction to the actual ground-state energy. The RVB state is probably made up of states

Fig. 10



SRO-breaking configurations of type (b).

having all possible values for the number of IPs between the maximum and small values, so (6), having half of the maximum, may be a good average. However, the above value for $\Delta E^{(2)}$ is rather large, and we feel certain that it would give an unreasonably low-lying ground state. There are two reasons for suspecting this. One of them is that the power expansion of $E_{cl}(4)$ suggests that the higher-order corrections to E_{gr} are not much smaller in magnitude than $\Delta E^{(2)}$, and alternating in sign. The other argument does not require the use of higher orders in perturbation theory, but relies on the apparent inadequacies of the wavefunction (6). Obviously, the 'solid background' rather diminishes the chances of coupling the same SRO-breaking state to different SRO states. Case (b), which considers the 'liquid part' of this state, may be more characteristic of the RVB state as a whole. If we suppose that each excited state couples to three SRO states and two of the matrix elements cancel, then, just as in case (b), we get a reduction by a factor of three when comparing to the naively estimated value of $\Delta E^{(2)}$. This would mean $\Delta E^{(2)} \sim -0.08\alpha^2 JN$. To find out whether this sort of cancellation really occurs, we examined the 'liquid part' (the central hexagon) of the cluster wavefunction represented in fig. 9. We found that out of the 24 corresponding excited states 12 are coupled to three SRO states and, roughly speaking, show the anticipated cancellation. However, six further states are coupled to two SRO states with no cancellation, and six other states only to one SRO state. This suggests that $0.08\alpha^2 JN$ is too small a value, and $(0.12-0.15)\alpha^2 JN$ may be better, but $|\Delta E^{(2)}|$ is probably not as high as $0.2\alpha^2 JN$.

To summarize, second order perturbation theory tends to put the ground state too low if we compare it with Anderson's (1973) cluster estimate. However, going further in perturbation theory is likely to restore a higher value, and there can be little doubt that perturbing from an RVB type state we can get lower than the estimated energy of the Néel state.

§ 5. DISCUSSION

The present work was motivated by a recent suggestion (Anderson 1973) that the $S=\frac{1}{2}$ antiferromagnets may not have Néel-type ground states and may be described more appropriately in terms of a quantum liquid formed of resonating singlet pair bonds. This suggestion gave fresh expression to old doubts founded on the early work of Bethe (1931) and Hulthén (1938) on the ground-state properties of the linear Heisenberg antiferromagnet. Bethe's

(1931) exact solution does not seem to show antiferromagnetic order, and Hulthén's (1938) work indicates that a linear combination of pair-bond wavefunctions is a natural choice for the ground state. Anderson (1973) applied Hulthén's method to set up variational wavefunctions for the triangular antiferromagnet in terms of singlet pair states. His cluster approximation gave a ground-state energy significantly lower than the value estimated for the Néel-type state, but did not give a clear idea of whether the ground state shows some type of ordering.

In order to explain a better idea of the ground-state properties we extended the investigation to the anisotropic triangular antiferromagnet described by the Hamiltonian (3) with $0 \leq \alpha \leq 1$. It was found that for $\alpha \ll 1$ the leading term in the ground-state energy (apart from the energy of the Ising ground state) is linear in α (see eqn. (5)). This ruled out the possibility that the ground state could be identical to the Néel-state shown in fig. 1 (*d*) which seems to be the most plausible choice for a quasi-classical state. Instead, the presence of short-range correlations, represented by the clusters in fig. 2, turned out to be relevant. The linear term in $E_{gr}(\alpha)$ is large enough (see eqns. (8)–(10)) to make this state competitive (see (11)) with the Néel state at $\alpha = 1$; and a cursory examination of the quadratic term (§ 4) suggests that this type of state may indeed be continued as ground state to the isotropic limit. Therefore we may tentatively identify it with the RVB state postulated by Anderson (1973). If this interpretation is valid, the RVB state has to be the ground state in the whole $0 < \alpha \leq 1$ interval and it is not intimately related to the description in terms of singlet pair states.

This touches upon another issue, whether the RVB state should be generally favourable for $S = \frac{1}{2}$ antiferromagnets. According to recent experiments (Gossard, diSalvo, Falconer, Rice, Voorhoeve and Yasuoka 1974) the Néel-type ground state is not infrequent; it has been found, e.g. in VF_4 , an $S = \frac{1}{2}$ quasi-two-dimensional square lattice antiferromagnet. Also, as is clear from § 2, the existence of this peculiar ground state is a consequence of two geometrical features of the triangular lattice: the 'zero point entropy' in the Ising limit (Wannier 1950) and the existence of the interchangeable pairs, i.e. that H^\pm has matrix elements between certain ground states of the Ising model. So there seems to be no reason for the appearance of an RVB type state in, e.g. a two-sublattice antiferromagnet, such as VF_4 . As far as we can see, the anomalous features of the other badly-behaving antiferromagnetic model, the linear chain, should have a different origin. The appearance of a gap for two branches of the triplet excitation spectrum for $\alpha > 1$ (des Cloizeaux and Gaudin 1966) seems to indicate that some form of DLRO is present in the correlation functions though this has not yet been proved. The ground state for the isotropic model is probably liquid-like, but in the case of the linear chain this is likely to be a continuation from the $\alpha \gg 1$ limit, not from $\alpha \ll 1$, as in the triangular lattice. The threefold degeneracy of the excitation spectrum for $\alpha \geq 1$ and the occurrence of a gap for two branches if $\alpha < 1$, seems to corroborate this suggestion.

Returning to the triangular case: while the energetical arguments are clearly in favour of a non-Néel-type ground state, we do not really know what type of order, if any, exists in it. The phase coherence guessed at in § 3 is probably present, and this would mean some form of Bose-condensation. Whether there is DLRO, remains undecided for the time being.

There being many SRO states mixed by H^\pm , the ground state should be the lower edge of a continuum of eigenstates for $0 < \alpha$. As the interchange of IPs does not change the z -component of the magnetization, at $\alpha = 1$ these states may correspond either to the $S^z = 0$ triplet branch, or to the singlet excitations. To change the magnetization we have to overcome a gap of the order of $J(1 - \alpha)$, so, should the RVB phase be found in nature, it would be characterized by a large low-temperature specific heat and a low susceptibility, at least in the z direction.

The chance of experimentally finding the RVB state, as interpreted here, seems to be rather small. We should have an undistorted, uniaxial $S = \frac{1}{2}$ antiferromagnet. Dichalcogenides of Nb and Ta could be considered, as these have fairly well-separated triangular transition metal ion layers. However, some of these (NbS_2 , NbSe_2 , TaSe_2) are metallic, so the Heisenberg model cannot apply. 1T-TaS_2 has three different phases, as established by resistivity measurements (Thompson, Gamble and Revelli 1971). The high-temperature phase is metallic and there is reason to suspect that the same is true of the intermediate phase (P. B. Allen, private communication). The low-temperature phase is probably semiconducting but the existence of the lattice distortion, the motivation for which is not entirely clear, interferes with the possible tendency for an RVB ground state. NbTe_2 and TaTe_2 are also distorted (Brown 1966). As having different nearest-neighbour distances results in removing the degeneracy of the SRO states, these materials also have to be ruled out as potential grounds for application of the RVB idea.

In summary, the interest of the present work lies mainly in giving an example where the antiferromagnetic Hamiltonian does not have a conventional antiferromagnetic ground state. However, just because the existence of this different ground state is so dependent upon the geometrical peculiarities of the triangular lattice, and on the absence of second-neighbour interactions, etc., which would tend to remove degeneracies, in realistic situations the assumption of a Néel-type state is further vindicated.

ACKNOWLEDGMENTS

The authors thank Mr. C. M. M. Nex for the help he has given with the numerical calculations. One of us (P.F.) expresses his gratitude for the permit of leave from Central Research Institute for Physics, Budapest, Hungary, and for the financial support and hospitality of the Cavendish Laboratory, Cambridge.

APPENDIX

In § 3 we guessed that if there are two different sequences of IP interchanges connecting two SRO states then these sequences contain either both an even or both an odd number of interchanges. In this appendix we demonstrate the validity of this statement for a special class of sequences connecting SRO states.

Let us suppose that the SRO states α and β differ only in that α has an up spin at site P and a down spin at site Q , while these are reversed in state β .

Let us suppose that there are two routes for getting from α to β always interchanging IPs only, containing m and n steps, respectively,

$$\left. \begin{aligned} \alpha \rightarrow \phi_1 \rightarrow \dots \rightarrow \phi_{m-1} \rightarrow \beta, \\ \alpha \rightarrow \psi_1 \rightarrow \dots \rightarrow \psi_{n-1} \rightarrow \beta. \end{aligned} \right\} \quad (\text{A } 1)$$

To each step there corresponds a line connecting the sites in the corresponding IP. Each route can be represented by a path connecting P and Q plus an arbitrary number of closed loops resulting in no net change. We disregard the complication caused by the closed loops. Let the two paths be $PR_1 \dots R_{m-1}Q$ and $PS_1 \dots S_{n-1}Q$. Here we shall consider only the simplest case when the spins along a path are parallel. So, for instance, if in the state α the sites R_1, \dots, R_{m-1} along the first route are all down spins, in the first step we interchange the PR_1 pair, then R_1R_2 , etc., thus letting the up spin jump from P to Q . If all the spins are up, the down spin jumps from Q to P . In both cases—and this is why this argument is not general, as we shall see—the order of pairs along a route is also the order in which we interchange them. The two sequences in (A 1) correspond to the two paths between P and Q , and together they form a closed polygon. (For the sake of simplicity we do not examine whether there are intersecting paths.) We have to prove that the number of the edges of this polygon (i.e. $n+m$) is even.

First let us consider what the $R_{i-1}R_iR_{i+1}$ angles can be. When the path consists of down spins, at the stage when the up spin has jumped to R_i , both $R_{i-1}R_i$ and R_iR_{i+1} have to be IPs. As an IP has to be embedded in a cluster like that in fig. 2, it is easy to make sure that two IPs have to form an angle of 120° . So all the angles of the polygon at the intermediate points of the paths have to be 120° or 240° .

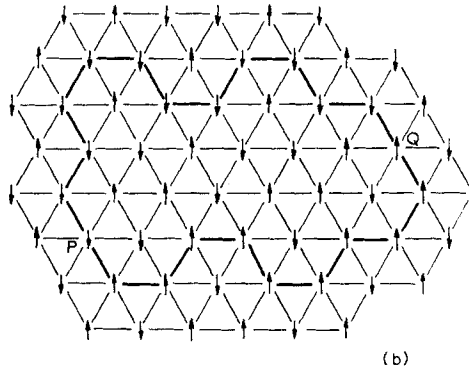
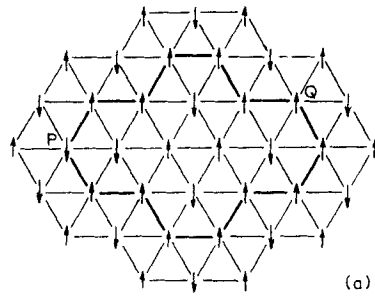
When both paths contain, let us say, down spins, at the outset both PR_1 and PS_1 have to be IPs, so their angle is also 120° . $S_{n-1}QR_{m-1}$ cannot be 60° for that would mean SRO breaking in α ; and it is easy to see that it cannot be 180° , either. Consequently, all the angles of the polygon are either 120° or 240° .

Now let us start out from the point P to R_1 and let us walk around the polygon. At each step we have to change direction by 60° and after $n+m-1$ steps we will be at 60° to our original direction. This can only result from making an odd number of steps, i.e. $n+m$ is even. One example is shown in fig. 11 (a).

The argument has to be slightly modified when the spins along the two paths are different, let us say \uparrow along $PR_1 \dots Q$ and \downarrow along $PS_1 \dots Q$ in α . We can easily check that the angles at P and Q become 180° . This obviously leaves the previous argument intact as an even number of direction changes have been removed. (One example of this situation is shown in fig. 11 (b).)

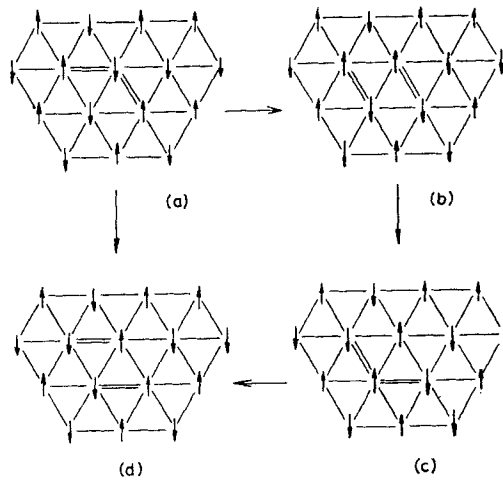
However, there can be ways of connecting α with β which do not fit into the previous picture. Figure 12 (a)–(d) shows a case when α and β differ only in the interchange of an IP. Either we can do immediately that, or we can go through the steps b – d . This latter route can be represented by a path which has an angle of 60° , does not have parallel spins in α , and which corresponds to an order of interchanges not identical to the order of pairs along the path. Our guess is not disproved here, as both routes have an odd (1 and 3, respectively

Fig. 11



Different paths connecting two states (a) both paths with the same spin, (b) an example when the spins for the two paths are opposite.

Fig. 12



The interchange of the horizontal IP in (a) can be done either immediately ($a \rightarrow d$) or via the interchanges $a \rightarrow b \rightarrow c \rightarrow d$.

Our guess is not disproved here, as both routes have an odd (1 and 3, respectively) number of interchanges but obviously there are intricate situations which are not easy to handle in a general way.

Further complications arise if we allow and restore changes which are not necessary for transferring the spins between P and Q and which can be represented by independent closed loops. If α and β differ at more than two sites the possibilities become even more numerous.

REFERENCES

- ANDERSON, P. W., 1973, *Mater. Res. Bull.*, **8**, 153.
 BETHE, H., 1931, *Z. Phys.*, **71**, 205.
 BROWN, B. E., 1966, *Acta crystallogr.*, **20**, 264.
 DES CLOIZEAUX, J., and GAUDIN, M., 1966, *J. Math. Phys.*, **7**, 1384.
 GOSSARD, A. C., DI SALVO, F. J., FALCONER, W. E., RICE, T. M., VOORHOEVE, F. M., and YASUOKA, H., 1974, *Solid St. Commun.*, **14**, 1207.
 HULTHÉN, L., 1938, *Ark. Mat. Astr. Fys.*, **26A**, 1.
 MARSHALL, W., 1955, *Proc. R. Soc. A*, **232**, 46.
 THOMPSON, A. H., GAMBLE, F. R., and REVELLI, J. F., 1971, *Solid St. Commun.*, **9**, 981.
 THOULESS, D. J., 1967, *Proc. phys. Soc.*, **90**, 243.
 WANNIER, G. H., 1950, *Phys. Rev.*, **79**, 357.